Biochemical and Biophysical Research Communications 656 (2023) 23–29

Contents lists available at ScienceDirect

Biochemical and Biophysical Research Communications

journal homepage: www.elsevier.com/locate/ybbrc

Contrasting the phospholipid profiles of two neoplastic cell lines reveal a high PC:PE ratio for SH-SY5Y cells relative to A431 cells

Espen Bariås [a], Martin Jakubec [a, b], Elise Førsund [a], Linda Veke Hjørnevik [a], Aurélia E. Lewis [a, *], Øyvind Halskau [a, *]

[a] Department of Biological Sciences, University of Bergen, Norway
[b] Department of Chemistry, University of Tromsø, Norway

ARTICLE INFO

Article history:
Received 17 February 2023
Received in revised form
3 March 2023
Accepted 8 March 2023
Available online 14 March 2023

Keywords:
Lipidomics
Plasma membrane
SH-SY5Y
NMR
LC-MS/MS
PC/PE ratio

ABSTRACT

Lipids have been implicated in Parkinson's Disease (PD). We therefore studied the lipid profile of the neuroblastoma SH-SY5Y cell line, which is used extensively in PD research and compared it to that of the A431 epithelial cancer cell line. We have isolated whole cell extracts (WC) and plasma membrane (PM) fractions of both cell lines. The isolates were analyzed with ^{31}P NMR. We observed a significant higher abundance of phosphatidylcholine (PC) for SH-SY5Y cells for both WC (55 ± 4.1%) and PM (63.3 ± 3.1%) compared to WC (40.5 ± 2.2%) and PM (43.4 ± 1.3%) of A431. Moreover, a higher abundance of phosphatidylethanolamine was detected for the WC of A431 compared to the SH-SY5Y. Using LC-MS/MS, we also determined the relative abundance of fatty acid (FA) moieties for each phospholipid class, finding that SH-SY5Y had high polyunsaturated FA levels, including arachidonic acid compared to A431 cells. When comparing our results to reported compositions of brain and neural tissues, we note the much higher PC levels, as well as very low levels of docosahexaenoic acid. However, relative levels of arachidonic acid and other polyunsaturated fatty acids were elevated, in line with what is desirable for a neural model system.

1. Introduction

Parkinson's Disease (PD) has been linked to changes in the neurological lipid composition [1]. It is thought that such changes could potentially contribute to the formation of harmful aggregates by α-Synuclein (α-Syn). This misfolding behaviour could in turn lead to a disruption of lipid metabolism [2], constituting a detrimental feedback mechanism between these misfolding diseases and the alteration of the lipidome. The investigation of these mechanisms would be helped by detailed knowledge of the lipidomes of relevant model systems. Clinical investigations and studies of animal models are resource intensive and limited by time, ethical considerations, and experimental options. Neurological cell lines, avoid these constraints and are generally accepted as valuable tools for the study of these diseases [3].

The lipid profiles of such cell lines, and in particular of their plasma membranes or organelles, are only recently beginning to be described in the scientific literature [4,5]. The SH-SY5Y cell line is a prime example of a cell line widely used in the study of neurological diseases, where lipids are increasingly being linked to disease progression [1,4]. It has been used to study several aspects of PD including toxicity induced by extracellular α-Syn [6], and the underling mechanisms and kinetics of α-Syn degradation [7,8]. The lipid profile of SH-SY5Y cells has not been extensively investigated, and has only been characterised in response to changes caused by Li^{2+}, and by neurotoxin treatments to induce cellular states relevant for PD [4,5,9]. The lipid composition of differentiated cells has also been investigated, with respect to fatty acid profile only [10]. The increased focus of lipids involvement in neurodegenerative

Abbreviations: α-Syn, α-Synuclein; NMR, Nuclear Magnetic Resonance; PD, Parkinson's Disease; ND, Neurodegenerative Diseases; PM, Plasma Membrane; PC, Phosphatidylcholine; PE, Phosphatidylethanolamine; PI, Phosphatidylinositol; PS, Phosphatidylserine; PG, Phosphatidylglycerol; SM, Sphingomyelin; CL, Cardiolipin; LPC, Lyso-Phosphatidylcholine; LPE, Lyso-Phosphatidylethanolamine; LPI, Lyso-Phosphatidylinositol; DiCH3PE, Dimethylphophsatidylethanolamine; AA, Arachidonic Acid; DHA, Ddocosahexaenoic Acid; FA, Fatty Acid.

* Corresponding authors. Department of Biological Sciences, University of Bergen, PB 7803, Bergen, N-5020, Norway.
E-mail addresses: aurelia.lewis@uib.no (A.E. Lewis), oyvind.halskau@uib.no (Ø. Halskau).

https://doi.org/10.1016/j.bbrc.2023.03.017

diseases (ND) raises the question whether the SH-SY5Y cell line is an optimal neuronal and ND model with regards to lipid composition.

We therefore chose the SH-SY5Y cell line as the primary target of our study and aimed to provide a comprehensive description of its phospholipid fraction. In such investigations, however, it is difficult to know whether notable observations are due to cell specialization, its neoplastic properties, cell culturing or methodology. We conducted a comparative lipidomic study, contrasting our results with another neoplastic cell line, A431, of epidermal origin. Neither cell lines are very well characterised with respect to their whole cell lipid composition, and little information regarding the composition of their plasma membrane (PMs) exists. ^{31}P NMR and LC-MS/MS were hence used to gain information about phospholipid composition and abundance as well as acyl chains for both whole cell and PM fractions, and significant differences were discussed in terms of lipid metabolism and suitability of SH-SY5Y as a model system for investigating lipid links to NDs.

2. Material and methods

2.1. Materials

The primary antibodies used in this study were as follows: Na^+/K^+ ATPase α (H-3) (Santa Cruz, SC-48345), Calnexin (Abcam, ab22595), β-Actin (Santa Cruz, SC-69879) and Lamin A/C (E-1) (Santa Cruz, SC-376248). The secondary anti-mouse or rabbit HRP-conjugated antibodies were from Thermo Fisher (G-21234 and G-21040). Lipase inhibitors (FIPI, U73122, and D609) were acquired from Tocris Bioscience Ltd. Dichloromethane was purchased from Thermo Fischer Scientific. Solutions for cell cultures, and all other chemicals were acquired from Millipore Sigma.

2.2. Cell culture and lipid isolation

The SH-SY5Y (obtained from DSMZ, ACC 209; Leibniz Institute) and A431 (obtained from Professor Arnesen) cell lines were cultured and harvested as described in Jakubec et al. [11]. The PM isolation protocol used in this study was an adaptation of the protocol by Costa and colleagues, and our previously published protocol [11–13]. Trypsinated cells were prepared as described in Ref. [11] and lysed with the hypotonic buffer used in Ref. [12]. The PM fractions were then isolated as described in Ref. [12]. The cell material for both whole cell and lipid extraction were frozen at −80 °C before being freeze-dried. The lipids obtained from the freeze-dried samples were isolated using a dichloromethane:methanol:water solution as described previously [11,14].

2.3. Western blot analysis

The purity of samples collected during PM isolation was checked using Western blot, as described in Jakubec et al. [11]. The membrane was incubated overnight at 4 °C with the primary antibodies for Na^+/K^+ ATPase α (1:5000), Calnexin (1:1000), β-Actin (1:1000) and Lamin A/C (E-1) (1:10000). A secondary HRP-conjugated antibody (1:25000, 1 h, RT) was used to detect the primary antibody. Detection of protein bands and gel visualization was achieved as in Jakubec et al. [11].

2.4. NMR and LC-MS/MS analysis

Fractions of the dried lipid material, extracted from whole cell and PM fractions as described above, were subjected to Accurate mass LC-MS and MS/MS on a Thermo Q-Exactive mass spectrometer and a Dionex Ultimate 3000 UPLC (ThermoFisher, USA). Other fractions of the extracted lipid material were resuspended with the Culeddu-Bosco "CUBO" solvent system [15], and the data was acquired at 300 K using a Bruker BioSpin NEO600 spectrometer. Both the LC-MS/MS and NMR were performed as previously described [11].

3. Results

3.1. Phospholipid composition of SH-SY5Y and A431 whole cell fractions

To investigate and compare the phospholipid content of SH-SY5Y and A431 cells, we isolated their whole cell fractions and analyzed them using quantitative ^{31}P NMR. First, NMR signals corresponding to phospholipids were identified based on their chemical shifts in the CUBO solvent [15]. NMR signals corresponding to PC, PE, $DiCH_3PE$, LPC, CL, SM, LPE, PI, PG, LPI and PS were identified in A431 extracts (Fig. 1A., lipid abbreviations explained in figure legend). Likewise, for the whole cell fractions of SH-SY5Y cells, the same lipids were identified except for LPE and LPI. The relative abundances of each lipid species were determined by integrating the deconvoluted peaks of the ^{31}P NMR spectra (Fig. 1A), and these abundances were then compared (Fig. 1B). Non-identified phosphorus signals were combined and referred to as Unidentified total (Utot). The most abundant lipid from the SH-SY5Y whole cell fractions was PC (55.0 ± 4.1%) followed by PE (14.4 ± 4.3%) (Fig. 1B and C). Similarly, the most abundant lipid in the A431 whole cell fractions was PC (40.5 ± 2.2%) followed by PE (26.4 ± 1.7%). The values for the remaining lipids are shown in Fig. 1C. We then compared the lipid abundance between the two cell lines and found significant differences for PC, PE, SM and PI, and found that the PC levels were significantly higher in the case of SH-SY5Y, while the levels of PE, SM, and PI were lower.

3.2. Phospholipid composition and abundance in SH-SY5Y and A431 plasma membranes

PM fractions were isolated from SH-SY5Y and A431 cells using centrifugation and the purity of the fractions was assessed with Western immunoblotting for the presence of markers for various subcellular locations (Fig. 2A). A substantial up-concentration of Na^+/K^+ ATPase (used as a PM marker) in the membrane pellets was achieved for both cell lines. Low amounts of Lamin A/C were detected for both cell lines in these fractions, indicating low nuclear contamination. Some contamination from ER membranes and the cytosol could not be avoided as Calnexin (used as an ER marker) and β-actin (a cytosol marker) were detected for both cell lines. We concluded that we obtained samples consisting predominantly of PM material and proceeded with determining the phospholipid abundances.

The PM fraction lipids were extracted and analyzed with ^{31}P NMR, as described for the whole cell fractions. From the PM fractions of both cell lines, the lipids identified were PC, PE, $DiCH_3PE$, LPC, SM, PI, and lower amounts of PS, CL and PG (Fig. 2B). The three most abundant phospholipids in the SH-SY5Y fractions were PC (63.3 ± 3.1%), PE (13.7 ± 4.4%) and PI (6 ± 1.6%). The same phospholipids were detected in the A431 PM fractions, with similar PI levels (7.7 ± 1.7%) but showed significantly lower PC levels (43.4 ± 1.3%) and higher PE levels (19.8 ± 3.9%) (Fig. 2C). The values for the remaining lipids are shown in Fig. 2C. Importantly, SH-SY5Y showed a significantly higher abundance of PC and lower abundance of SM.

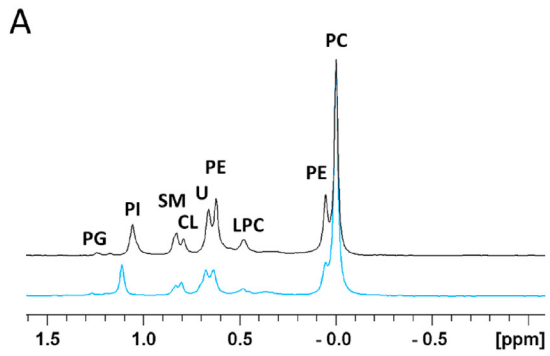

C

Phospho-lipids	Abundance SH-SY5Y	Abundance A431
PC	55.0 ± 4.1	40.5 ± 2.2 *
PE	14.4 ± 4.3	26.4 ± 1.7 *
CL	4.0 ± 3.7	4.8 ± 2.4
SM	2.3 ± 0.4	7.0 ± 1.1 *
PI	7.2 ± 0.9	9.4 ± 0.5 *
PG	0.9 ± 0.4	2.6 ± 2.2
PS	10.2 ± 8.1	3.9 ± 4.7
Utot	6.9 ± 10.8	4.8 ± 3.3

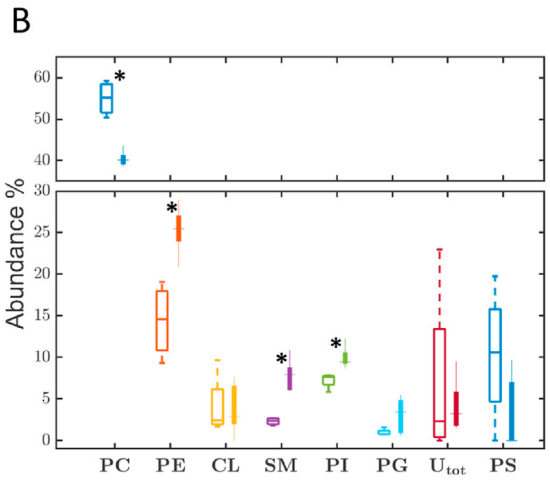

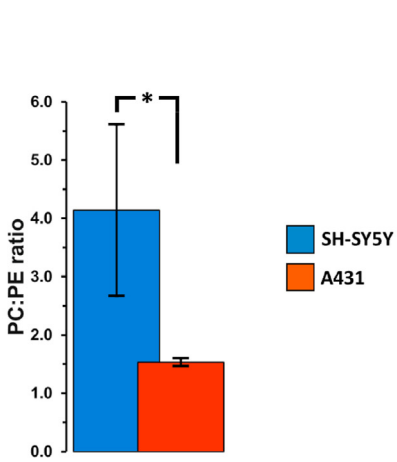

Fig. 1. ^{31}P NMR spectra and phospholipid abundance of whole cell fractions from SH-SY5Y and A431 cells. A) ^{31}P spectrum of an SH-SY5Y (Blue) and A431 (Black) whole cell samples. The different peaks in spectrum represents a specific phospholipid and the abundance are dependent on the area occupied and the height and sharpness of the peak. The most abundant lipid, PC, was used to calibrate the axis and set to 0 ppm. B) Box plot representing the distribution of the abundance of each phospholipid in the individual samples after deconvolution of the ^{31}P NMR spectra. The unfilled boxes on the left side of each phospholipid represents the SH-SY5Y samples (n = 4) and filled boxes on the right are A431 samples (n = 4). Utot represents the peaks that could not be identified in the ^{31}P spectra. C) The average abundance of each phospholipid from SH-SY5Y and A431 fractions with standard deviation based on the population added. Abbreviations: Phosphatidylcholine (PC), Lysophosphatidylcholine (LPC), Phosphatidylethanolamine (PE), Cardiolipin (CL), Sphingomyelin (SM), Phosphatidylinositol (PI), Phosphatidylglycerol (PG), Phosphatidylserine (PS), Unidentified (U), Unidentified total (Utot). D) PC:PE ratios. Ratios from four measurements were calculated for each cell type; the average and standard deviations of the ratios are shown as bars and error bars, respectively. For panels B, C and D, the «*» indicates where a significant difference was observed (two-tailed Welch *t*-test, $p \leq 0.05$). (For interpretation of the references to color in this figure legend, the reader is referred to the Web version of this article.)

3.3. Acyl chain abundances in whole cell and plasma membrane fractions

We also sought to identify which acyl chains are attached to the different phospholipids. After isolating the lipids from whole cell fractions, samples were also analyzed using our previously developed iterative exclusion LC/MS method and LipMat script [11,16]. Acyl chains were identified for all the glycerophospholipids isolated from the whole cell fractions for both cell lines, except for PG, which was only detected in A431 cells (Table 1). From the SH-SY5Y whole cell fractions, relative abundances were acquired for two acyl chains for PC, 14:0 (41 ± 20.3%) and 16:0 (41 ± 20.3%). The most abundant acyl chains were 18:0 (42.1 ± 9.8%) for PE, 18:0 (38.8 ± 18%) and 20:4 (47.4 ± 17.1%) for PI, and 18:0 (48.5 ± 14.9%) and 18:1 (38.3 ± 20.5%) for PS.

In the A431 whole cell fractions, the most abundant acyl chains were 16:0 for PC (50 ± 28.3%) and 18:0 for PI species (29.3 ± 3.3%). In contrast, unsaturated acyl chains were the most abundant lipid moieties in the other glycerophospholipids, 18:1 for PE (41.4 ± 3.1%), PS (41.9 ± 9.1%) and the only acyl chains quantified for PG were 18:1 (50 ± 11.6%). The polyunsaturated fatty acid (PUFA) 20:4 was detected for PE (6.5 ± 1.7%) and PI (11.9 ± 5.2%) and 22:6 was detected for PE (1.4 ± 0.4%) and PI (0.3 ± 0.09%). The remaining values for the acyl chains for the whole cell fractions of both cell lines are shown in Table 1.

For the PM fractions, acyl chains were identified for PC, PE, PI, PS and PG for both cell lines (Table 2). The most abundant acyl chains in the SH-SY5Y PM fractions were 18:1 (35.7 ± 4.9%) for PC, 18:1 (25.1 ± 4.8%) for PE, 18:1 (27.0 ± 6.7%) for PI and 18:0 (39.4 ± 6.3%) for PS. 20:4 was detected with PC (4.5 ± 0.1%), PE (18.0 ± 6.2%) and PI (20.2 ± 2.4%). 22:6 was only detected for PE (2.6 ± 1.6%). In the A431 PM fractions the most abundant acyl chain was 16:0 (47.8 ± 15.8%) for PC and 18:1 (47.7 ± 4.9%) for PE. The highest abundance for PI was 18:1 (27.0 ± 6.7%) and the same for PS (17.6 ± 12.2%). 20:4 was detected for PE (18.0 ± 6.2%) and PI (20.2 ± 2.4%). The rest of the values for the acyl chains in the SH-SY5Y and A431 PM fractions are shown in Table 2.

3.4. Abundance of SFA, MUFA and PUFA in whole cell and PM fractions

From the data acquired from the LC-MS/MS analysis of the PM fractions, the abundance of saturated FA (SFA), monounsaturated FA (MUFA) and PUFA was identified (Fig. 3). For the whole cell

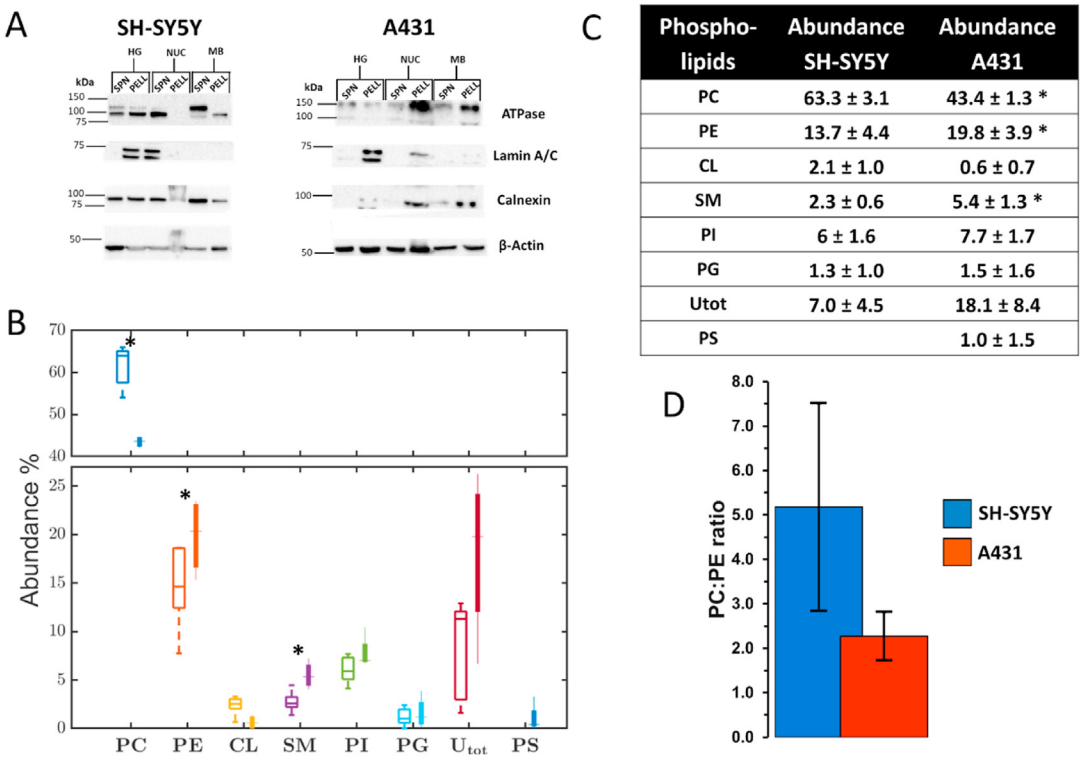

Fig. 2. Purity of the plasma membrane fractions and their phospholipid composition and abundance. A) Fractions collected from the isolation of PM from SH-SY5Y and A431 cells were sonicated and centrifuged, and the resulting pellets (PELL) and supernatants (SPN) were resolved on a 10% SDS-PAGE. This was then transferred to a nitrocellulose membrane and incubated with different antibodies to check the purity. The following antibodies were used: ATPase (Plasma membrane), Lamin A/C (Nucleus), Calnexin (ER), β-Actin (Cytoplasmic). B) PM fractions that were deemed pure enough were analyzed with ^{31}P NMR to identify the phospholipid composition. The box plots represent the abundance of each phospholipid in the different samples after deconvolution of the ^{31}P NMR spectra. The open boxes on the left side of each phospholipid represents the SH-SY5Y samples (n = 4) and colored boxes on the right are A431 samples (n = 4). C) The average abundance of each phospholipid from SH-SY5Y and A431 fractions with standard deviation based on the population added. The «*» indicates where a significant difference was observed (two-sided Welch *t*-test, $p \leq 0.05$). Abbreviations: Homogenate (HG) Supernatant (SPN), Pellet (Pell) Nuclei (NUC), Membrane (MB), Phosphatidylcholine (PC), Phosphatidylethanolamine (PE), Cardiolipin (CL), Sphingomyelin (SM), Phosphatidylinositol (PI), Phosphatidylglycerol (PG), Phosphatidylserine (PS), Unidentified total (Utot). D) PC:PE ratios. Rations from four measurements were calculated for each cell type; the average and standard deviations of the ratios are shown as bars and error bars, respectively. No significant difference was observed (two-tailed Welch *t*-test, p = 0.085).

Table 1
Relative abundance of fatty acids identified for the phospholipids isolated in SH-SY5Y and A431 whole cell fractions. The number of samples for SH-SY5Y and A431 were n = 6 and n = 4, respectively. The relative abundance is given in % with standard deviations.

FA	SH-SY5Y WC				A431 WC				
	PC	PE	PI	PS	PC	PE	PI	PS	PG
14:0	41.0 ± 20.3								
16:0	41.0 ± 20.3				50 ± 28.3	11.1 ± 4.2	7.0 ± 1.5	9.5 ± 3.9	
16:1						4.0 ± 0.8	5.6 ± 2.8	3.2 ± 0.1	
17:1							2.1 ± 1		
18:0		42.1 ± 9.8	38.8 ± 18.0	48.5.4 ± 14.9		12.9 ± 4.2	29.3 ± 3.3	33.2 ± 12.7	
18:1			10.7 ± 6.4	38.3 ± 20.5		41.4 ± 3.1	24.0 ± 2.1	41.9 ± 9.1	50 ± 11.6
18:2						6.8 ± 2.9	8.1 ± 5.4		
20:1						2.5 ± 1.3	5.5 ± 2		
20:3							3.2 ± 1.9	2.2 ± 1.0	
20:4			47.4 ± 17.1			6.5 ± 1.7	11.9 ± 5.2		
22:6						1.4 ± 0.4	0.3 ± 0.09		
Others	17.9	57.8	2.9	13	50	13.1	2.6	9.7	50

fractions the abundance of MUFA were higher for A431 (47.2 ± 4.6%) compared to SH-SY5Y cells (23.3 ± 7.2%). The opposite was observed for PUFA with a higher abundance for SH-SY5Y (39.6 ± 2.2%) compared to A431 (19.4 ± 6.6%). The SFA abundance was similar for both cell lines as seen in Fig. 3A. A significant difference was observed for MUFA and PUFA ($p < 0.05$, two-tailed Welch *t*-test). The abundance of SFA, MUFA and PUFA for the PM fractions were identified as for the whole cell fractions. Like the whole cell fractions, the SH-SY5Y cells had a higher abundance of PUFA and lower MUFA compared to A431 cells. The differences in MUFA and PUFA were significant ($p < 0.05$, two-tailed Welch *t*-test). The SFA abundance was similar for both cell lines, which can be seen in Fig. 3B.

4. Discussion

Our approach allowed us to extract sufficient PM lipid material for ^{31}P NMR analyses, and as such addressed a problem

Table 2
The relative abundance of fatty acids identified for the different phospholipids detected in the SH-SY5Y and A431 plasma membrane fractions. The number of samples for SH-SY5Y and A431 were n = 4 and n = 3, respectively. The relative abundance is given in % with standard deviations.

FA	SH-SY5Y PM					A431 p.m.				
	PC	PE	PI	PS	PG	PC	PE	PI	PS	PG
13:1	0.4 ± 0.2									
14:0	1.9 ± 0.1									
16:0	21.1 ± 2.8	4.0 ± 2.0	5.4 ± 2.7			47.8 ± 15.8	13.7 ± 7.6	17.8 ± 4.5	21.6 ± 14.2	
16:1	20.8 ± 6.2						5.3 ± 2.6	4.3 ± 1.1	1.5 ± 0.05	30.2 ± 4.2
16:2	0.6 ± 0.1	1.4 ± 0.1								
17:0			1.2 ± 0.1							
17:1	1.3 ± 0.5	3.3 ± 1.2								
18:0	11.2 ± 3.3	24.5 ± 3.1	17.5 ± 3.7	39.4 ± 6.3			19.5 ± 6.7	22.2 ± 2.1	8.4 ± 3.9	
18:1	35.7 ± 4.9	25.1 ± 4.8	27.0 ± 6.7	17.6 ± 12.2	40.6 ± 15.4	39.5 ± 20.9	47.7 ± 4.9	22.5 ± 3.6	49.3 ± 8.9	31.8 ± 4.8
18:2								7.5 ± 0.8		
18:3							0.7 ± 0.07			
19:1		5.3 ± 1								
20:3			25.6 ± 5.7					2.7 ± 0.8		
20:4	4.5 ± 0.1	18.0 ± 6.2	20.2 ± 2.4				2.1 ± 0.7	3.9 ± 0.6		
22:3		0.5 ± 0.2								
22:6		2.8 ± 1.6								
Others	2	14.6	2.8	42.8	59.3	12.5	10.7	18.7	19	37.9

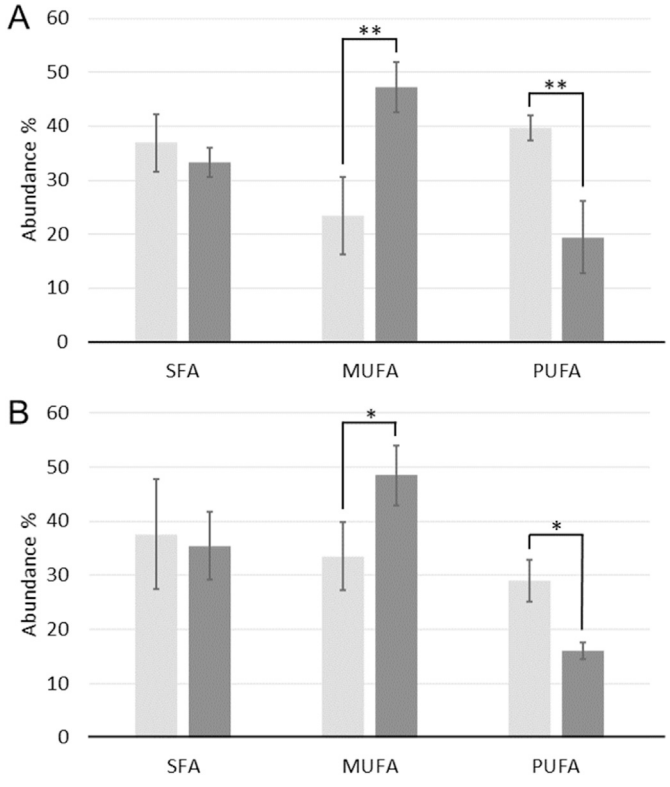

Fig. 3. *Abundance of saturated, monounsaturated, and polyunsaturated fatty acids in Whole cell and PM fractions.* A) Average abundance in % of saturated fatty acids (SFA), monounsaturated fatty acids (MUFA) and polyunsaturated (PUFA) in whole cell fractions for A431, represented in black (n = 4) and SH-SY5Y is in grey (n = 4). B) Average abundance of FA categories in PM fractions with standard deviations based on the whole population added. A431 represented in black (n = 3) and SH-SY5Y in grey (n = 4). The «*» and «**» indicate where a significant difference was observed (two-tailed Welch *t*-test, $p \leq 0.05$ and $p \leq 0.005$ respectively).

encountered in our earlier study [11]. The nuclear contaminations were removed in large parts from the PM fractions, but endoplasmic reticulum (ER) contamination, as indicated by Calnexin, persisted in the fractions after attempts at optimization. The presence of Calnexin has been observed in other studies [11,17]. The difficulty of removing ER could be related to the membrane contact sites that connects the PM to the ER [18]. Similarly, mitochondrial contamination has also been reported and was observed in the ^{31}P NMR analysis in the form of CL and PG, lipids that are enriched in this organelle [19]. Removal of the mitochondrial contamination proved difficult, so instead, samples presenting high contents of CL and PG were rejected from further analysis.

The analysis of the phospholipid composition of the whole cell fraction revealed that there was a significant difference in the abundance of PC, PE, PI and SM between the SH-SY5Y and A431 cell lines. The abundance of PC, PE and PI in the A431 cells was similar to that reported for other epithelial cell lines [20,21]. For SH-SY5Y the SM abundance was similar to our previous study of the same cell line [11], but lower compared to A431. However, we note that the abundance of these phospholipids in the SH-SY5Y differs from reported brain composition [22,23], with a higher abundance of PC and PI and lower amounts of PE and SM. The PC abundance reported for neurons isolated from rat brain (54.2%) is similar to our results but higher compared to rabbit (46.8%). The neurons isolated from rat and rabbit had a PE abundance between 27.1% and 31%, which is higher than our values. For PI, we see a higher abundance compared to rat (6.0%) and rabbit neurons (5.6%), while SM abundance was lower compared to rat (4.4%) and rabbit (7.9%) [24,25].

For the PM fractions of both cell lines, we were able to detect a significant difference in the abundance of PC and SM. PC abundance in SH-SY5Y cells was similar to what we observed previously [11]. This measure is also higher than what is usually observed for the PM of mammalian cells (40–50% for rat liver cells, baby hamster kidney cells) [19,26,27]. Interestingly, the measured SH-SY5Y PC values are much higher compared to that of human white matter (30.2%) and grey matter (38.9%). The PM lipid composition of human neurons has not been well described, but relative to synaptic PMs derived from rat and other neuroblastoma cultures suggests that the PC abundance of the PM of SH-SY5Y cells is higher [28,29]. Another significant difference was the low PM abundance of SM in the SH-SY5Y fractions compared to A431. Unlike our previous study there were no increase of SM, and it was lower than in A431 PM fractions. The change in PM isolation methodology could have caused this, but the lower SM abundance is also observed for whole cell extracts.

Although not significant at $p = 0.085$, we comment that the abundance of PE in the SH-SY5Y PM fractions was lower compared to A431, our previous study, and the PM of other mammalian cells [19,26,27]. The abundance is also lower than in the human brain

and that of synaptic and synaptosomal PMs [22]. Notably, it is more similar to the PE abundance of a neuroblastoma cell line of mouse origin [28], tentatively suggesting that neuroblastoma cell lines share this feature. The abundance of PE is however much lower than for tumours [30], and is most likely related to the unavailability of ethanolamine in the cell medium. The PE abundance is also much lower than white matter (34.1%) and grey matter (42.2%). This difference is also observed when compared to the PE (35.6%) abundance of the whole human brain [22].

The high abundance of PC and the simultaneous low PE abundance seems to be a robust and specific trait of the PM of SH-SY5Y cells. To maintain this state, it is likely that there is an upregulation of PC synthetic pathways, including the *de novo* Kennedy pathway, the Land's cycle or the trimethylation of PE. The dysregulation of choline metabolism is one of the hallmarks that are observed in most cancers [31]. Furthermore, it is reported that SH-SY5Y cells ability to take up choline is enhanced and is mainly carried out by choline transporter-like protein 1 [32,33]. Neuroblastomas have been reported to have high concentrations of phosphocholine, indicating a possible upregulation of choline kinase (CK) [34]. Notably, the activity of CKα in SH-SY5Y cells was shown to decrease in PD-mimicking disease models [35].

From the PC and PE abundance we saw that the PC/PE ratio was unusually high in the PM, with 5:1, compared to the 2:1 ratio that are reported in the literature [19,26,27]. The same ratio was also observed for the whole cell fractions indicating that the ratio is consistent between whole cell and PM. Changes in this ratio have been reported to affect the integrity of cell membranes leading to cell damage, energy metabolism of organelles, growth and cell survival [36,37]. Related to this, cell activities such as membrane fusion, fission and budding could be affected since PE modulates membrane curvature [38,39]. Possibly in line with this, abnormal PC/PE ratios have been observed in non-alcoholic steatohepatitis and malignant neoplastic cells with metastases [40,41].

In analysing the composition of FA, we were especially interested by the relative abundance of arachidonic acid (AA) and docosahexaenoic acid (DHA), which are both enriched in the human brain [22]. From the LC-MS/MS data, a low relative abundance of DHA was detected in PE in the SH-SY5Y PM fractions. This value was also low compared to our last study ($\approx$3% vs $\approx$ 16%) [11]. This is also lower than what has been reported in parts of the human brain, which is enriched with DHA, and to PM fractions of neuronal origin from rat brain [29,42,43]. The low DHA abundance is most likely caused by the low availability of DHA and the necessary precursor 18:3 in the cell medium. Cell media have been shown to have an impact on FA composition, and adding extra DHA has shown to increase its content in SH-SY5Y cells [10,44,45]. No DHA was detected as FA for the phospholipids in the SH-SY5Y whole cell and A431 PM fractions, and only low abundances was detected for PE and PI in the A431 whole cell fractions.

Unlike DHA, AA was detected as one of the main FAs for PE, PC and PI from the SH-SY5Y PM fractions. The relative abundance of AA, as a FA of PE and PC, was similar to our previous study and to that of grey matter and white matter as previously reported [42,46]. Compared to synaptosomal and synaptic PMs from rat brain we saw that the AA composition of PC and PE match closely [29,43]. That AA was detected for PC in SH-SY5Y cell is interesting since AA is not the most abundant FA associated with PC in the brain. AA was also detected as one of the FAs for PE in the A431 PM fractions, but in lower relative abundance than in SH-SY5Y PM fractions. A notable observation was the high abundance of AA, as a part of PI. This is interesting since AA has been reported as one of the main FAs of PI in the brain [22]. Compared to grey matter and synaptosomal PM, the amount of AA is low. However, the abundance of AA as a component of PI is very similar to that of white matter [42,43]. It is also higher than in the A431 PM. fractions and seems to be another specific trait of the SH-SY5Y PM, along with the AA composition for PE.

The total and relative amounts of PUFA and MUFA present in neural tissue is relevant for misfolding diseases [47–49]. The higher abundance of PUFA in the SH-SY5Y cells compared to A431 cells in our study suggest that SH-SY5Y cell membranes tend towards more fluid and looser lipid packing. However, A431 cells has a higher abundance of MUFAs, possibly providing overall fluidity in a similar manner. The high abundance of PUFA is surprising since it is reported that cultured cells usually have an unnatural high abundance of MUFA [45].

From these results, we see that the lipid profile of the neoplastic cell line SH-SY5Y differs to that of neuronal cells and the brain, the abundance of PC and PE being the most notable differences as well as the low abundance of DHA as a FA moiety of PE. However, the SH-SY5Y cell line matches reported values for AA distribution of relevant neural tissue quite well. Moreover, the high total PUFA amounts for this cell line is similar. Although factors such as origin, passage number, medium quality, and degree of cell line proliferation are factors that influence lipidomic results, our comparison to A431 cells allows us to conclude that the SH-SY5Y features reported here are characteristic of this cell line. Despite some non-neurological lipid characteristics, it can serve as a model system for lipid-related research, provided that results associated with PC and DHA are not given undue weight.

Author contributions

Formulated scientific questions: EB, AEL, ØH. Designed experiments: EB, ØH. Established PM isolation method: EB, AEL, LVH. Collected and analyzed NMR and MS data: EB, MJ. Prepared whole cell samples: EF, EB. All other lab work: EB. Prepared figures EB, MJ, ØH. Data curation and supervision: AEL, ØH. Manuscript drafts: ØH, EB. Read, commented, and approved final manuscript version: all. Funding was obtained by ØH.

Declaration of competing interest

The authors declare that they have no known competing financial interests or personal relationships that could have appeared to influence the work reported in this paper.

Acknowledgements

The work was financed through the Research Council of Norway grant NFR240063. The authors thank the staff at the NNP Bergen node for facilitating the NMR work, which was also in part supported by Bergen Research Foundation, Sparebankstiftinga Sogn og Fjordane and the Research Council of Norway through the Norwegian NMR Platform, NNP (226244/F50). We thank Thomas Stevenson and Sushma Grellscheid for critically reading the manuscript, and Thomas Arnesen for providing the A431 cell line.

References

[1] H. Xicoy, B. Wieringa, G.J.M. Martens, The role of lipids in Parkinson's disease, Cells 8 (2019), https://doi.org/10.3390/cells8010027.
[2] I. Alecu, S.A.L. Bennett, Dysregulated lipid metabolism and its role in α-synucleinopathy in Parkinson's disease, Front. Neurosci. 13 (2019) 328.
[3] D.F. Lázaro, M.A.S. Pavlou, T.F. Outeiro, Cellular models as tools for the study of the role of alpha-synuclein in Parkinson's disease, Exp. Neurol. 298 (2017) 162–171, https://doi.org/10.1016/j.expneurol.2017.05.007.
[4] H. Xicoy, J.F. Brouwers, O. Kalnytska, et al., Lipid analysis of the 6-hydroxydopamine-treated SH-SY5Y cell model for Parkinson's disease, Mol. Neurobiol. 57 (2020) 848–859, https://doi.org/10.1007/s12035-019-01733-3.
[5] C.L. Sanchez, C.L. Souders, C.J. Pena-Delgado, et al., Neurotoxicity assessment

of triazole fungicides on mitochondrial oxidative respiration and lipids in differentiated human SH-SY5Y neuroblastoma cells, Neurotoxicology 80 (2020) 76–86, https://doi.org/10.1016/j.neuro.2020.06.009.
[6] S. Emadi, S. Kasturirangan, M.S. Wang, et al., Detecting morphologically distinct oligomeric forms of α-synuclein, J. Biol. Chem. 284 (2009) 11048–11058, https://doi.org/10.1074/jbc.M806559200.
[7] X. Liangliang, H. Yonghui, E. Shunmei, et al., Dominant-positive HSF1 decreases alpha-synuclein level and alpha-synuclein-induced toxicity, Mol. Biol. Rep. 37 (2010) 1875–1881, https://doi.org/10.1007/s11033-009-9623-2.
[8] M.C. Bennett, J.F. Bishop, Y. Leng, et al., Degradation of α-synuclein by proteasome, J. Biol. Chem. 274 (1999) 33855–33858, https://doi.org/10.1074/jbc.274.48.33855.
[9] B.T. Layden, A.M. Abukhdeir, C. Malarkey, et al., Identification of Li^+-binding sites and the effect of Li^+ treatment on phospholipid composition in human neuroblastoma cells: a ^{7}Li and ^{31}P NMR study, Biochim. Biophys. Acta, Mol. Basis Dis. 1741 (2005) 339–349, https://doi.org/10.1016/j.bbadis.2005.07.004.
[10] L.M. Reynolds, C.F. Dalton, G.P. Reynolds, Phospholipid fatty acids and neurotoxicity in human neuroblastoma SH-SY5Y cells, Neurosci. Lett. 309 (2001) 193–196, https://doi.org/10.1016/S0304-3940(01)02071-7.
[11] M. Jakubec, E. Bariås, F. Kryuchkov, et al., Fast and quantitative phospholipidomic analysis of SH-SY5Y neuroblastoma cell cultures using liquid chromatography–tandem mass spectrometry and ^{31}P nuclear magnetic resonance, ACS Omega 4 (2019) 21596–21603, https://doi.org/10.1021/acsomega.9b03463.
[12] E.M. Costa, B.B. Hoffmann, G.H. Loew, Opioid agonists binding and responses in SH-SY5Y cells, Life Sci. 50 (1992) 73—81, https://doi.org/10.1016/0024-3205(92)90199-y.
[13] T. Maeda, K. Balakrishnan, S. Qasim Mehdi, A simple and rapid method for the preparation of plasma membranes, Biochim. Biophys. Acta, Biomembr. 731 (1983) 115–120, https://doi.org/10.1016/0005-2736(83)90404-2.
[14] S. Furse, M. Jakubec, F. Rise, et al., Evidence that Listeria innocua modulates its membrane's stored curvature elastic stress, but not fluidity, through the cell cycle, Sci. Rep. 7 (2017) 1–11, https://doi.org/10.1038/s41598-017-06855-z.
[15] M. Bosco, N. Culeddu, R. Toffanin, et al., Organic solvent systems for ^{31}P nuclear magnetic resonance analysis of lecithin phospholipids: applications to two-dimensional gradient-enhanced 1H-detected heteronuclear multiple quantum coherence experiments, Anal. Biochem. 245 (1997) 38–47, https://doi.org/10.1006/abio.1996.9907.
[16] J.P. Koelmel, N.M. Kroeger, E.L. Gill, et al., Acquisition with automated exclusion list generation, J. Am. Soc. Mass Spectrom. 28 (2018) 908–917, https://doi.org/10.1007/s13361-017-1608-0.
[17] H. Ogiso, M. Taniguchi, T. Okazaki, Analysis of lipid-composition changes in plasma membrane microdomains, J. Lipid Res. 56 (2015) 1594–1605, https://doi.org/10.1194/jlr.M059972.
[18] W.A. Prinz, Bridging the gap: membrane contact sites in signaling, metabolism, and organelle dynamics, J. Cell Biol. 205 (2014) 759–769, https://doi.org/10.1083/jcb.201401126.
[19] S.E. Horvath, G. Daum, Lipids of mitochondria, Prog. Lipid Res. 52 (2013) 590–614, https://doi.org/10.1016/j.plipres.2013.07.002.
[20] M.L. Dória, C.Z. Cotrim, C. Simões, et al., Lipidomic analysis of phospholipids from human mammary epithelial and breast cancer cell lines, J. Cell. Physiol. 228 (2013) 457–468, https://doi.org/10.1002/jcp.24152.
[21] R. Magny, N. Auzeil, E. Olivier, et al., Lipidomic analysis of human corneal epithelial cells exposed to ocular irritants highlights the role of phospholipid and sphingolipid metabolisms in detergent toxicity mechanisms, Biochimie 178 (2020) 148–157, https://doi.org/10.1016/j.biochi.2020.07.015.
[22] A. Naudí, R. Cabré, M. Jové, et al., in: M.J.B.T.-I.R. of N. Hurley (Ed.), Chapter Five - Lipidomics of Human Brain Aging and Alzheimer's Disease Pathology, Omi. Stud. Neurodegener. Dis. Part B, Academic Press, 2015, pp. 133–189, https://doi.org/10.1016/bs.irn.2015.05.008.
[23] J. Choi, T. Yin, K. Shinozaki, et al., Comprehensive analysis of phospholipids in the brain, heart, kidney, and liver: brain phospholipids are least enriched with polyunsaturated fatty acids, Mol. Cell. Biochem. 442 (2018) 187–201, https://doi.org/10.1007/s11010-017-3203-x.
[24] W.T. Norton, T. Abe, S.E. Poduslo, et al., The lipid composition of isolated brain cells and axons, J. Neurosci. Res. 1 (1975) 57–75, https://doi.org/10.1002/jnr.490010106.
[25] A. Hamberger, L. Svennerholm, Composition of gangliosides and phospholipids of neuronal and glial cell enriched fractions, J. Neurochem. 18 (1971) 1821–1829, https://doi.org/10.1111/j.1471-4159.1971.tb09587.x.
[26] Y. Yang, M. Lee, G.D. Fairn, Phospholipid subcellular localization and dynamics, J. Biol. Chem. 293 (2018) 6230–6240, https://doi.org/10.1074/jbc.R117.000582.
[27] G. van Meer, D.R. Voelker, G.W. Feigenson, Membrane lipids: where they are and how they behave, Nat. Rev. Mol. Cell Biol. 9 (2008) 112–124, https://doi.org/10.1038/nrm2330.
[28] N.M. Gulaya, G.L. Volkov, V.M. Klimashevsky, et al., Changes in lipid composition of neuroblastoma C1300 N18 cell during differentiation, Neuroscience 30 (1989) 153–164, https://doi.org/10.1016/0306-4522(89)90361-8.
[29] C. Cotman, M.L. Blank, A. Moehl, et al., Lipid composition of synaptic plasma membranes isolated from rat brain by zonal centrifugation, Biochemistry 8 (1969) 4606—4612, https://doi.org/10.1021/bi00839a056.
[30] F. Podo, Tumour phospholipid metabolism, NMR Biomed. 12 (1999) 413–439, https://doi.org/10.1002/(SICI)1099-1492(199911)12:7<413::AID-NBM587>3.0.CO;2-U.
[31] K. Glunde, Z.M. Bhujwalla, S.M. Ronen, Choline metabolism in malignant transformation, Nat. Rev. Cancer 11 (2011) 835–848, https://doi.org/10.1038/nrc3162.
[32] M. Inazu, Choline transporter-like proteins CTLs/SLC44 family as a novel molecular target for cancer therapy, Biopharm. Drug Dispos. 35 (2014) 431–449, https://doi.org/10.1002/bdd.1892.
[33] T. Yamada, M. Inazu, H. Tajima, et al., Functional expression of choline transporter-like protein 1 (CTL1) in human neuroblastoma cells and its link to acetylcholine synthesis, Neurochem. Int. 58 (2011) 354–365, https://doi.org/10.1016/j.neuint.2010.12.011.
[34] S.E. Kohe, C.D. Bennett, S.K. Gill, et al., Metabolic profiling of the three neural derived embryonal pediatric tumors retinoblastoma, neuroblastoma and medulloblastoma, identifies distinct metabolic profiles, Oncotarget 9 (2018) 11336–11351, https://doi.org/10.18632/oncotarget.24168.
[35] A.T. Baykal, M.R. Jain, H. Li, Aberrant regulation of choline metabolism by mitochondrial electron transport system inhibition in neuroblastoma cells, Metabolomics 4 (2008) 347–356, https://doi.org/10.1007/s11306-008-0125-3.
[36] J.N. van der Veen, J.P. Kennelly, S. Wan, et al., The critical role of phosphatidylcholine and phosphatidylethanolamine metabolism in health and disease, Biochim. Biophys. Acta, Biomembr. 1859 (2017) 1558–1572, https://doi.org/10.1016/j.bbamem.2017.04.006.
[37] G. Tasseva, H.D. Bai, M. Davidescu, et al., Phosphatidylethanolamine deficiency in mammalian mitochondria impairs oxidative phosphorylation and alters mitochondrial morphology, J. Biol. Chem. 288 (2013) 4158–4173, https://doi.org/10.1074/jbc.M112.434183.
[38] J.E. Vance, G. Tasseva, Formation and function of phosphatidylserine and phosphatidylethanolamine in mammalian cells, Biochim. Biophys. Acta Mol. Cell Biol. Lipids 1831 (2013) 543–554, https://doi.org/10.1016/j.bbalip.2012.08.016.
[39] D. Marsh, Lateral pressure profile, spontaneous curvature frustration, and the incorporation and conformation of proteins in membranes, Biophys. J. 93 (2007) 3884–3899, https://doi.org/10.1529/biophysj.107.107938.
[40] I. Dobrzyńska, B. Szachowicz-Petelska, S. Sulkowski, et al., Changes in electric charge and phospholipids composition in human colorectal cancer cells, Mol. Cell. Biochem. 276 (2005) 113–119, https://doi.org/10.1007/s11010-005-3557-3.
[41] Z. Li, L.B. Agellon, T.M. Allen, et al., The ratio of phosphatidylcholine to phosphatidylethanolamine influences membrane integrity and steatohepatitis, Cell Metabol. 3 (2006) 321–331, https://doi.org/10.1016/j.cmet.2006.03.007.
[42] L. Svennerholm, Distribution and fatty acid composition of phosphoglycerides in normal human brain, J. Lipid Res. 9 (1968) 570–579.
[43] W.C. Breckenridge, G. Gombos, I.G. Morgan, The lipid composition of adult rat brain synaptosomal plasma membranes, Biochim. Biophys. Acta, Biomembr. 266 (1972) 695–707, https://doi.org/10.1016/0005-2736(72)90365-3.
[44] M. Treen, R.D. Uauy, D.M. Jameson, et al., Effect of docosahexaenoic acid on membrane fluidity and function in intact cultured Y-79 retinoblastoma cells, Arch. Biochem. Biophys. 294 (1992) 564–570, https://doi.org/10.1016/0003-9861(92)90726-D.
[45] P.L. Else, The highly unnatural fatty acid profile of cells in culture, Prog. Lipid Res. 77 (2020), 101017, https://doi.org/10.1016/j.plipres.2019.101017.
[46] J.S. O'Brien, E.L. Sampson, Fatty acid and fatty aldehyde composition of the major brain lipids in normal human gray matter, white matter, and myelin, J. Lipid Res. 6 (1965) 545–551.
[47] R. Sharon, I. Bar-Joseph, M.P. Frosch, et al., The formation of highly soluble oligomers of α-synuclein is regulated by fatty acids and enhanced in Parkinson's disease, Neuron 37 (2003) 583–595, https://doi.org/10.1016/S0896-6273(03)00024-2.
[48] T. Viennet, M.M. Wördehoff, B. Uluca, et al., Structural Insights from Lipid-Bilayer Nanodiscs Link α-Synuclein Membrane-Binding Modes to amyloid, Nature Publishing Group, 2018, https://doi.org/10.1038/s42003-018-0049-z.
[49] C. Galvagnion, J.W.P. Brown, M.M. Ouberai, et al., Chemical properties of lipids strongly affect the kinetics of the membrane-induced aggregation of α-synuclein, Proc. Natl. Acad. Sci. U. S. A 113 (2016) 7065–7070, https://doi.org/10.1073/pnas.1601899113.